The Effect of the Sixth Sulfur Ligand in the Catalytic Mechanism of Periplasmic Nitrate Reductase

N. M. F. S. A. CERQUEIRA,[1] P. J. GONZALEZ,[1] C. D. BRONDINO,[2] M. J. ROMÃO,[1] C. C. ROMÃO,[3] I. MOURA,[1] J. J. G. MOURA[1]

[1]*REQUIMTE, Departamento de Química, Centro de Química Fina e Biotecnologia, Faculdade de Ciências e Tecnologia, Universidade Nova de Lisboa, 2829-516 Caparica, Portugal*

[2]*Departamento de Física, Faculdad de Bioquímica e Ciencias Biológicas, Universidad Nacional del Litoral, 3000ZAA Santa Fé, Argentina*

[3]*Instituto de Tecnologia Química e Biológica, Universidade Nova de Lisboa, Av da República, EAN, 2780-157, Oeiras, Portugal*

Received 11 November 2008; Accepted 26 February 2009
DOI 10.1002/jcc.21280
Published online in Wiley InterScience (www.interscience.wiley.com).

Abstract: The catalytic mechanism of nitrate reduction by periplasmic nitrate reductases has been investigated using theoretical and computational means. We have found that the nitrate molecule binds to the active site with the Mo ion in the +6 oxidation state. Electron transfer to the active site occurs only in the proton-electron transfer stage, where the Mo^V species plays an important role in catalysis. The presence of the sulfur atom in the molybdenum coordination sphere creates a pseudo-dithiolene ligand that protects it from any direct attack from the solvent. Upon the nitrate binding there is a conformational rearrangement of this ring that allows the direct contact of the nitrate with Mo^{VI} ion. This rearrangement is stabilized by the conserved methionines Met141 and Met308. The reduction of nitrate into nitrite occurs in the second step of the mechanism where the two dimethyl-dithiolene ligands have a key role in spreading the excess of negative charge near the Mo atom to make it available for the chemical reaction. The reaction involves the oxidation of the sulfur atoms and not of the molybdenum as previously suggested. The mechanism involves a molybdenum and sulfur-based redox chemistry instead of the currently accepted redox chemistry based only on the Mo ion. The second part of the mechanism involves two protonation steps that are promoted by the presence of Mo^V species. Mo^{VI} intermediates might also be present in this stage depending on the availability of protons and electrons. Once the water molecule is generated only the Mo^{VI} species allow water molecule dissociation, and, the concomitant enzymatic turnover.

 J Comput Chem 00: 000–000, 2009

Key words: nitrate reductase; catalytic mechanism; molybdenum; DFT

Introduction

Nitrate reductases are mononuclear Mo-containing enzymes, where the molybdenum atom is coordinated to one or two pterin molecules. The coordination sphere is completed with a restricted range of atoms, namely oxygen (from oxo, hydroxo, water, serine or aspartic acid molecules) or sulfur (cysteine). These enzymes are widely found in eukaryotes (Plants, Algae, Fungi, Yeast) and prokaryotes (Archaea, Bacteria) organisms.[1,2]

Taking into account the mononuclear Mo containing enzymes classification, these enzymes belong to the DMSO reductase family with the exception of the assimilatory eukaryotic nitrate reductases, which are part of the sulfite oxidase family[3] (see Fig. 1). Despite the differences observed in the active site topology and the atoms present in the molybdenum coordination sphere, all enzymes catalyze a common and important biological reaction that reduces nitrate (NO_3^-) into nitrite (NO_2^-), involving an atom abstraction. In each cycle two electrons and two protons are consumed, and in the end one water molecule is produced. The process is only activated in the presence of nitrate and is repressed by oxygen.

$$NO_3^- + 2H^+ + 2e^- \rightarrow NO_2^- + H_2O \quad E^\circ = +420\,mV$$

Additional Supporting Information may be found in the online version of this article.

Correspondence to: J. J. G. Moura; e-mail: jose.moura@dq.fct.unl.pt

Contract/grant sponsor: Fundação para a Ciência e Tecnologia (FCT); contract/grant numbers: POCTI/35736/99, POCI/QUI/57641/2004, POCI2010, SFRH/PD/5105/2006

Contract/grant sponsors: FEDER, GRICES

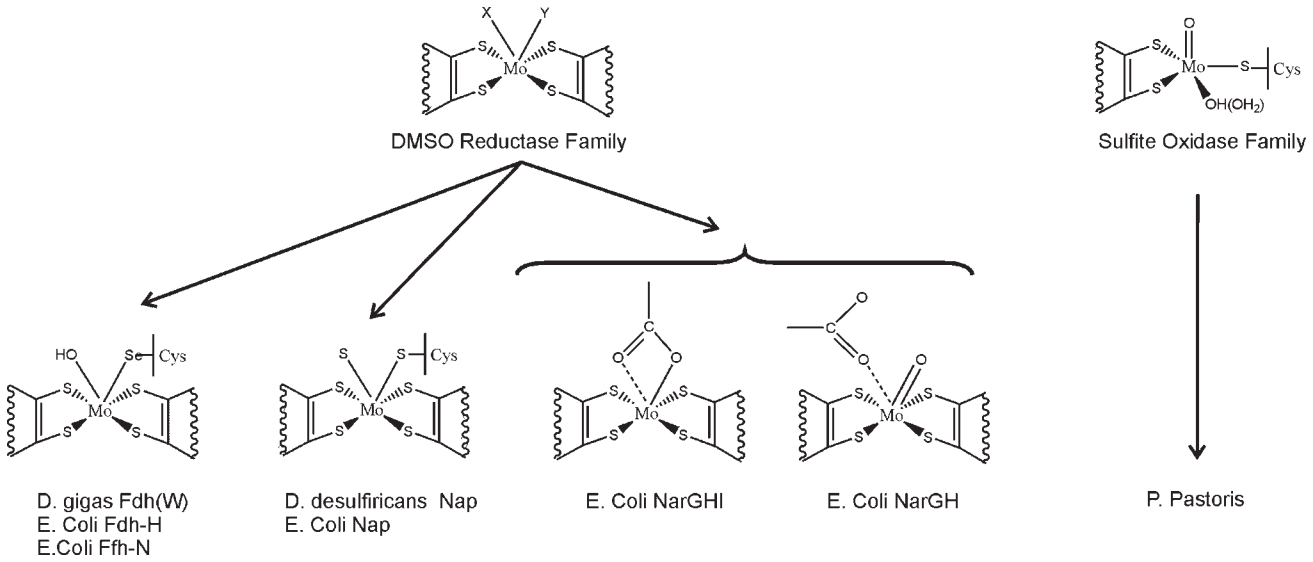

Figure 1. Active site structure of two mononuclear Mo enzyme families in which nitrate redutases can be found.

This reaction is widely used in nature either for assimilatory ammonification, denitrification or dissimilatory ammonification.[2,4] The first process is a crucial step in the nitrogen cycle. The assimilatory nitrate reductase is the first enzyme involved in a sequence of concomitant reductive steps that promote the incorporation of nitrogen into biomass, accommodating in this way the bioavailability of NO_3^- that is essential to plants, algae, fungi, archaea and bacteria. Nitrate reductases have also a key role in the first steps of denitrification and dissimilatory ammonification. The first process is used by some microorganisms to generate energy for cellular function, through the reduction of nitrate into a series of intermediate gaseous nitrogen oxide products. It only occurs under special conditions, especially when oxygen, a more energetically favorable electron acceptor, is depleted. The dissimilatory ammonification is less common than denitrification and involves the reduction of nitrate to ammonium. It is used by some bacteria for energy generation under anoxic conditions.

To date, there are several examples of nitrate reductases characterized structurally from eukaryotic[5] and prokaryotic organisms. The crystal structures of the periplasmic nitrate reductases from *Desulfovibrio desulfuricans* (*Dd*NapA),[6] *Rhodobacter sphaeroides* (*Rs*NapAB)[7] and *E. coli* (*Ec*NapA)[8] show high similarities in protein fold and active sites. These three enzymes contain a *bis*-molybdopterin guanine dinucleotide (*bis*-MGD) active site and a [4Fe-4S] cluster in their catalytic subunits. The Mo atom is coordinated by two dithiolene ligands from the two MGD molecules, a γ-sulfur from a cysteine and a sixth ligand, which was originally proposed to be a hydroxyl/water molecule.[6] A recent detailed structural study of the active site of NapA from *Desulfovibrio desulfuricans* has shown that the sixth ligand of the molybdenum is a sulfur atom instead of oxygen.[9] This type of coordination is not new, and has already been observed in formate dehydrogenase from *Desulfovibrio gigas* (*Dg*Fdh)[10] and *Escherichia coli* (*Ec*Fdh-H),[11] in which the main difference is that the cysteine sulfur is replaced by a Se atom from a selenocysteine residue. The presence of the sulfur atom near Cys140 creates a pseudo-dithiolene ligand that interacts very closely with the molybdenum atom. This new rearrangement protects the molybdenum atom from the solvent.

The new active site topology with an additional sulfur ligand demanded a revision of the currently accepted mechanism and several alternatives were proposed on the basis of the reanalysis of the structural data of the Dd NapA.[9]

We have now used theoretical and computational tools to revise the catalytic mechanism of nitrate reductase using, as basis, the new crystallographic data from NapA from *Desulfovibrio desulfuricans*[9] as well as the experimental observations reported to date.

Methods

The coordinates of the protein were taken from the 1.99 Å resolution X-ray structure of *Desulfovibrio desulfuricans* nitrate reductase (PDB code: 2v3v).[9]

The model chosen to study the catalytic mechanism of NAP includes a molybdenum bis-dimethyl dithiolene complex, in which the ligands represent a portion of the cofactor. The coordination sphere of the Mo centre was completed with a sulfur atom, and an SCH_3 group that was chosen to mimic the Cys140 residue. The model was subsequently completed with the conserved Gln346 and the neighbor Gly345 that completes the Nap active site.

To keep the optimized structures close to the experimental ones, some atoms were frozen from their corresponding positions in the X-ray structure. The atoms that were fixed are marked with an asterisk in Figure 2. This model was then used

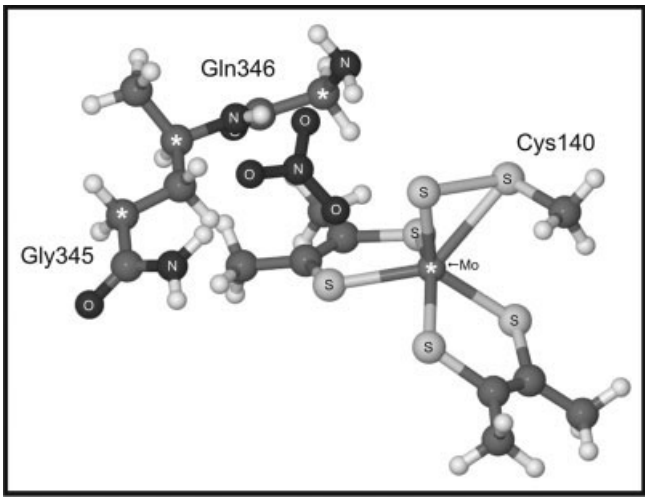

Figure 2. Model used to study the catalytic mechanism of Nap (frozen atoms are marked with a white asterisk).

to build three systems with different Mo oxidation states: Mo(IV) (charge −4, spin multiplicity 1), Mo(V) (charge −3, spin multiplicity 2) and Mo(VI) (charge −2, spin multiplicity 1).

All geometry optimizations were performed with Gaussian 03,[12] applying density functional methods. Becke's three-parameter exchange functional was used together with the functional of Lee et al.[13–16] (B3LYP) as implemented in Gaussian and the 6-31G(d) basis set. For the geometry optimizations and subsequent frequency calculations the Lanl2DZ effective core potential (Los Alamos effective core potential plus double zeta)[17] basis set was used for the molybdenum ion.

All the geometry optimizations were performed in the following way. Our first step involved the search of the transition state, starting from a structure similar to the transition state. This is generally obtained with a previous scan when the reaction coordinated that we are interested in, is shortened or stretched. Once the transition state was located, the connected minima, the reactants and the products, were determined through internal reaction coordinate (IRC) calculations. In all cases, the geometry optimizations and the stationary points were obtained with standard Gaussian convergence criteria. The transition state structures were all verified by vibrational frequency calculations, and have exactly one imaginary frequency with the correct transition vector (Although it is well known that performing frequency calculations on constrained systems is inaccurate, from the mathematical point of view, this procedure gives a reasonable approximation when compared to the free system). The atomic charges and spin densities were calculated using a Mulliken population analysis.

Further, single point energy calculations were computed with the B3LYP functional (6-311++G(2p,2d)) and the lanl2dzp effective core potential basis set. Relativistic effects are implicitly covered through the use of these effective core potentials. Relative energies include unscaled zero point vibrational energies as obtained from B3LYP/Lanl2Dz frequencies. A polarized continuum model was employed, referred as C-PCM, as implemented in Gaussian03, to calculate the final energies. In this approach, the continuum is modeled as a conductor, instead of a dielectric. This simplifies the electrostatic computations, and corrections are made a posteriori for dielectric behavior. A dielectric constant of $\varepsilon = 4$ was chosen to describe the protein environment of the active site in accordance with previous suggestions.[18–20]

Results and Discussion

The currently accepted mechanism for periplasmic nitrate reductases was originally proposed based on the information from the original X-ray structure of *Dd*NapA.[6]

In this proposal the enzyme was assumed to have the active site in the Mo^{VI} form. In the presence of the electron donor, the hexacoordinated Mo^{VI} would be reduced to a pentacoordinated Mo^{IV} in a two electron transfer reaction mediated by the [4Fe-4S] center. The nitrate molecule would thereafter bind to Mo^{IV} in the vacant position left by the hydroxyl/water ligand and then two electrons would be transferred from the Mo^{IV} to the nitrate molecule with the concomitant release of nitrite and regeneration of the Mo^{VI} form of the enzyme (Scheme 1).

Although this mechanism is in line with the accepted reaction of Mo enzymes,[21] it conflicts with several experimental data obtained in the last years.[8,9,22]

The most significant difference is the presence of a sulfur atom bound to the molybdenum center, instead of an oxygen as well as the presence of a partial disulfide bond as reported in the crystallographic reanalysis.[6,9] This new active site topology forms a pseudo-dithiolene ligand that protects molybdenum atom from the solvent, and from any direct interaction of molecules such as nitrate. Moreover, spectropotentiometric[8,23,24] studies have also revealed that nitrate binding to the active site should only involve Mo^{V} and Mo^{VI} species, and not Mo^{IV} species, as previously thought, due to the low potential of $Mo^{V} \rightarrow Mo^{IV}$ (below −400 mV *vs*. SHE) that would turn its presence almost negligible in physiological conditions. Furthermore, EPR studies[22] under rapid turnover conditions yield a new rhombic Mo^{V} signal detectable after electron donor (reduced methyl viologen) shortage, indicating that the two-electron reaction formerly proposed[6] is not correct.

In the present paper we propose to revise this mechanism and try to elucidate by computational means the involvement of the new identified sulfur in this process, along with all the other experimental data. The results are divided in three sections: In the first one, the new structural data will be analyzed and the presence of the sulfur atom in the molybdenum center will be discussed. In the second section, we will propose what should be the most favorable oxidation state of molybdenum when no nitrate molecules are present. In this section, the oxidation state of the molybdenum center and the configuration of the active site in the initial state will be discussed. These results will then be used, in the third section, to study the catalytic mechanism that involves the nitrate reduction into nitrite, and the most favorable pathway will be presented. The last section will be focused on the protonation of the oxo-group left after nitrite release that leads to the formation of a water molecule and regeneration of the active site.

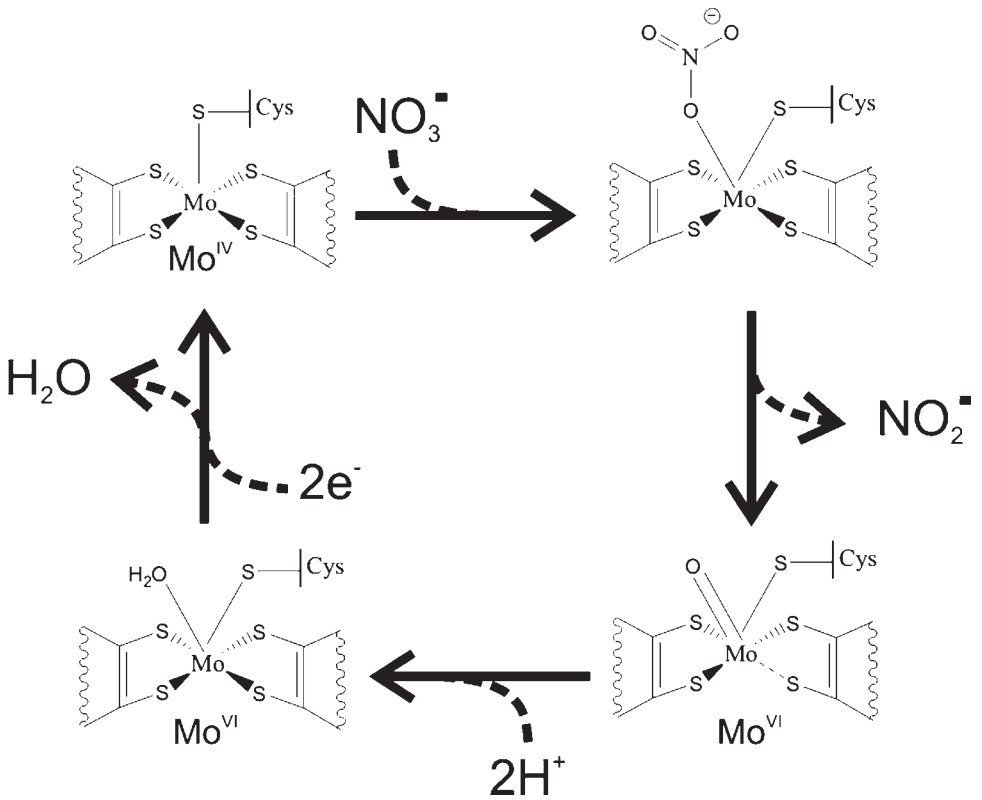

Scheme 1. Catalytic mechanism adapted from the proposal by Dias et al.[6]

Structural Information of the Nitrate Reductase Active Site

The X-ray structure of the periplasmic nitrate reductase from *D. desulfuricans* (*Dd*Nap) is a monomeric polypeptide of the α/β-fold type, with a molecular mass of 80 kDa. This protein is divided in four domains (I-IV), three of which are formed by non-contiguous stretches of the polypeptide chain. All four domains are involved to variable extents in cofactor binding, but only one domain is responsible for the binding of the [4Fe-4S] cluster center that is located at the periphery of the molecule, and serves as an electron pump. The bis-molybdopterin guanosine dinucleotide cofactor is embedded across the interior of the protein, and interacts with the residues from all four domains through several hydrogen bonds.

The spatial arrangement of domains II and III creates a funnel-like cavity at their interface, focused towards the molybdenum center and located ca. 12 Å below the protein surface. The access to the molybdenum center is assisted by the presence of several charged aminoacid residues, namely, Asp155, Glu156, Arg709, Arg354, which conduct, through hydrogen bonds and electrostatic interactions, the nitrate molecule, from the solvent to the molybdenum center. The analysis of the D*d*NapA X-ray structure reflects this issue[9] revealing that near the molybdenum center only one nitrate molecule can fit and that the direct contact with molybdenum center is precluded. Near the active site the funnel becomes very tight and can only fit small molecules.

Using the Caver algorithm[25,26] we have also found two additional channels that also point towards the molybdenum center (see Fig. 3). These two channels are located on the interface of domains I and II and between domains II and IV, and might be used by the enzyme as water channels for supplying the protons that are required for enzyme turnover, or to remove water molecules that are generated during the catalytic process from the active site.

The molybdenum, present in the active site, is hexacoordinated with a distorted trigonal prismatic geometry. The coordination sphere around the molybdenum atom includes four thiol ligands from the two pterinic molecules with Mo-S bond distances at an average distance of 2.4 Å, one sulfur ligand from Cys-140 with a Mo-S bond length of 2.3 Å, and a sulfur at 2.3 Å. Previous crystallographic studies suggested that the coordination sphere of the metal was completed by a hydroxo/water molecule, but recent new diffraction data allowed a more complete analysis and has revealed the presence of a sulfur atom instead.[9] The presence of the anionic sulfur near Cys140 creates a pseudo-dithiolene ligand that interacts very closely with the molybdenum atom. Near Cys140 there are two conserved methionine residues, Met141 and Met308 (see Fig. 4), that may help the stabilization of the negative charge that is spread between the molybdenum, the sulfur anion and Cys140.

The presence of the pseudo-dithiolene ligand partly blocks the active site and narrows even more the substrate accessing funnel, preventing by this way any direct contact of the Mo with the solvent or any small molecule such as nitrate. This means that the direct contact of the nitrate molecule with the molybde-

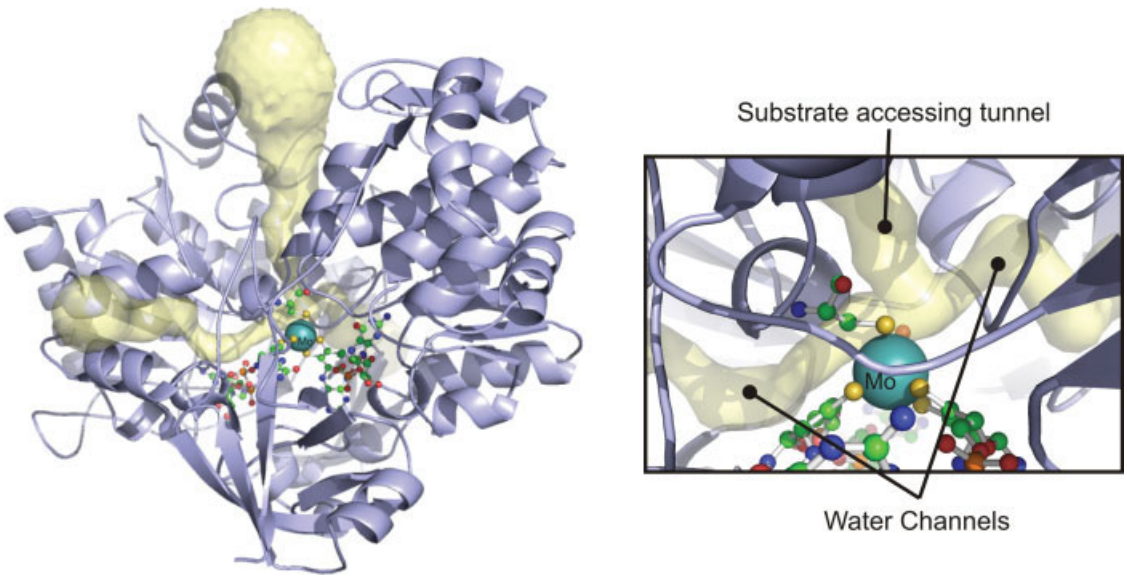

Figure 3. Crystal structure of Nap (PDB: 2jio) with the tunnels (yellow colored) identified by CAVER.[25,27]

num ion may be precluded, contrarily to what was previously proposed.[6] However, a change in the oxidation state of the molybdenum ion may induce a conformational rearrangement of the pseudo-dithiolene ligand and mask the true reductive pathway. To clarify this issue, we studied the conformation of the metallic center varying the oxidation state of the molybdenum ion. The results are presented in the next section together with the discussion of what should be the most favorable oxidation state of the molybdenum ion *in vivo* at the initial state.

Oxidation State of the Molybdenum Atom and the Conformational Rearrangement of the Active Site

To study the properties of the active site in the three possible oxidation states and to clarify the former proposal[9] whether the pseudo-dithiolene ligand undergoes a conformational rearrangement when the molybdenum changes the oxidation state, we built three models containing the molybdenum atom in the three oxidation states, Mo^{IV} (singlet state), Mo^{V} and Mo^{VI} (Fig. 5).

In all the optimized structures, the molybdenum complex shows a distorted prismatic trigonal complex, with an average Mo-S(dithiolene) distance of 3.5 Å No significant conformational rearrangement was observed in the pseudo-dithiolene ligand. In the Mo^{IV} minimum the Mo-Cys140, and the Mo-S bond lengths have values around 2.6 Å and 2.3 Å, respectively, and in the Mo^{V} and Mo^{VI} models, about 2.5 Å and 2.2 Å, respectively. These values show that higher oxidation states of molybdenum lead to the shortening of these bond lengths. Looking at the charge distribution of these atoms we can also conclude that, the charge concentration decreases within the sulfur and S-Cys as the oxidation states of the Mo increases. These two effects influence the type of interaction established between the sulfur anion and the sulfur of Cys140, despite the fact that the distance between them remains almost identical in all three models (3.5 Å). Therefore, in lower Mo oxidation states these atoms tend to interact through an anionic disulfide bridge, but this character decreases as the Mo oxidation state increases to become a standard dissulfide bridge. Nevertheless, and independently of the molybdenum oxidation state, the pseudo-dithiolene ligand remains attached to the molybdenum ion preventing the direct interaction with water molecules. These results also show that substrate binding must involve a molybdenum-sulfur redox chemistry.[9]

From a detailed analysis of the currently available literature it is known that the Mo^{VI} species are often found either in

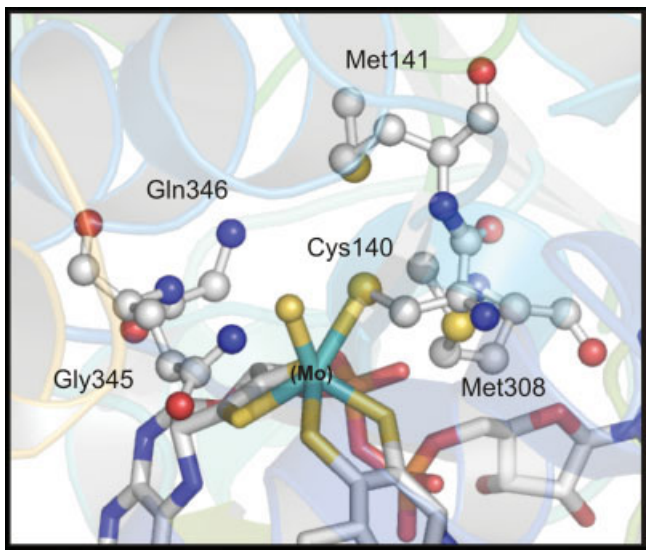

Figure 4. Active site topology of the D.desulfuricans Nap (PDB: 2jio).[9]

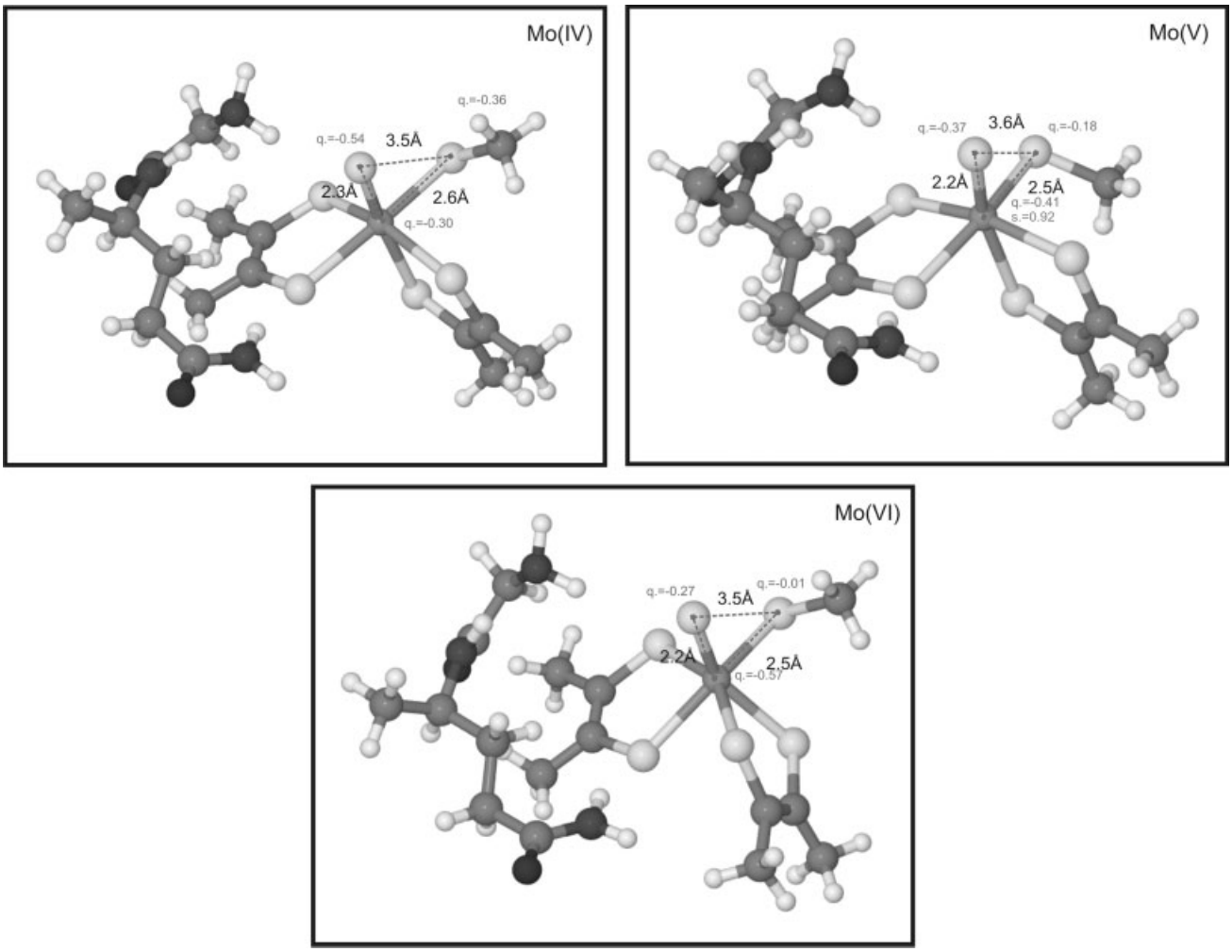

Figure 5. Optimized models of the Nap active site region containing the molybdenum atom in three oxidation states, Mo^{IV}, Mo^{V}, and Mo^{VI}.

nitrate reductases or in other Mo-*bis*-MGD-dependent reductases such as the DMSO reductase.[1] However, due to the possibility of photo-reduction during X-ray data collection, the redox state of the molybdenum atom cannot be known with certainty, and therefore the redox states Mo^{IV}, Mo^{V} and Mo^{VI} can be potential intervenients.

Taking into account the spectropotentiometric and PFV studies performed by several authors in different periplasmic nitrate reductases,[8,22–24] the presence of Mo^{IV} ion seems unlikely to occur *in vivo*, as the redox potential of the Mo^{V}/Mo^{IV} couple is very low (below −500 mV vs SHE) and consequently it would be hardly obtained with physiologic electron donors. However, the potential range over which the Mo^{VI} is reduced to Mo^{V} state for several Naps is between +200 mV and −200 mV,[7,8,24,28] except for Nap from *Desulfovibrio desulfuricans*, whose redox couple has an electrochemical potential below −500 mV[2]. Therefore both Mo^{5+} and Mo^{6+} can be found in equilibrium at physiologic conditions. This means that the substrate could not interact with the Mo^{4+} ion as previously thought, but with a more oxidized form instead.

The Catalytic Reduction Mechanism of Nitrate into Nitrite

The reduction of nitrate into nitrite involves a standard oxo-transfer reaction in which the molybdenum atom is believed to have a relevant role. In the new coordination sphere of molybdenum, the presence of the anionic sulfur atom creates a partial disulfide bond with Cys140 that blocks the access of the nitrate molecule to the molybdenum ion, either in Mo^{V} or Mo^{VI}. This means that upon nitrate binding, concomitant redox interplay of molybdenum, sulfur and Cys140, must be involved to promote the reduction of nitrate into nitrite. Two possibilities can be drawn for the catalytic mechanism: a second coordination sphere or a first coordination sphere mechanism, similarly to what was proposed before[9] (Scheme 2). The presence of the pseudo-dithiolene ligand, closely tight to the molybdenum ion, suggests a

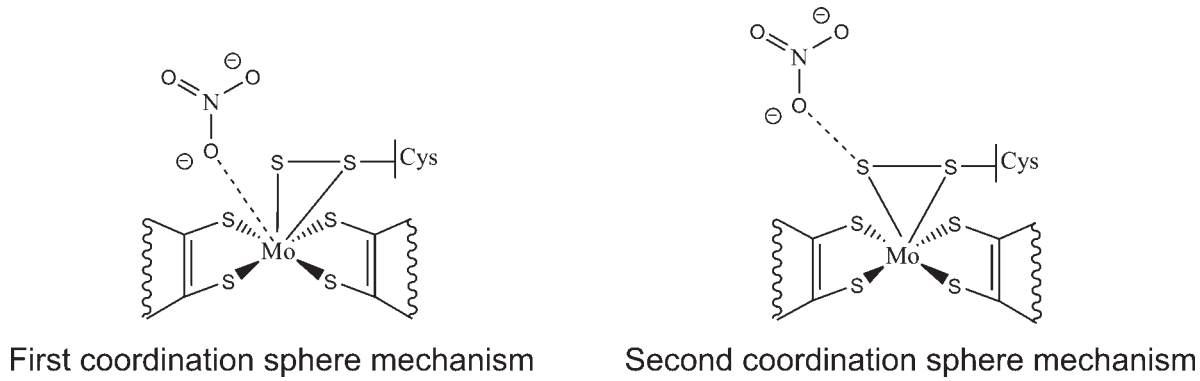

Scheme 2. First and second coordination sphere mechanisms - working hypothesis.

second coordination sphere type mechanism. In this case the nitrate molecule would only be able to interact directly with the sulfur atom because the methionines present near the active site may block any direct interaction with the sulfur of Cys140.

In the first coordination sphere mechanism, the nitrate molecule has to bind directly to the molybdenum ion. The former is in line with previous experimental[8,9] and theoretical[29,30] mechanistic suggestions, but requires a conformational rearrangement of the pseudo-dithiolene ligand to facilitate the access of the nitrate molecule to the molybdenum center.

To study which type of reaction would be the most favorable we created a model with the Mo-bis(dimethyl dithiolene) complex, in which the ligands represent a portion of the cofactor. As before, an SCH_3 group was chosen to mimic the Cys140 residue and together with the sulfur atom it completes the coordination sphere of the Mo ion.

As Mo^{V} and Mo^{VI} can be found in equilibrium *in vivo*, and in our calculations they lead to different pathways, we will present both mechanisms independently, discuss them at the end, and the most favorable pathway will be presented.

Oxo-Transfer Reaction Mediated by Mo^{VI} bis(dithiolene)

Step 1 (Scheme 3) The geometry optimization of the Mo^{VI} model kept the essential geometric features and the hydrogen-bonding network observed in the crystal structure. The optimized equilibrium geometry of the reactants is close to a distorted prismatic trigonal complex, with an average Mo-S(dithiolene) distance of 2.5 Å. The nitrate molecule adopts a planar geometry with the closest oxygen atom at 4.0 Å away from the molybdenum ion and is stabilized by several hydrogen bounds provided by Gln346 and Gly454. The sulfur atom from Cys140 is bound to the molybdenum atom (2.8 Å) and is connected to the sulfido through a standard disulfide bridge (2.4 Å). The sulfido is also bound to the molybdenum atom (2.4 Å) and is 2.6 Å away from the nitrate molecule. From the analysis of the Mulliken population it can be seen that the charge is spread mostly through the Mo atom (−0.41 a.u.), the dithiolene ligands (−0.77 a.u.), and the nitrate molecule (−0.53 a.u.).

In the transition state, the negatively charged nitrate molecule (−0.54 a.u.) gets closer to the molybdenum complex (3.57 Å) and stays at 2.8 Å from the sulfur atom (Fig. 6). The proximity

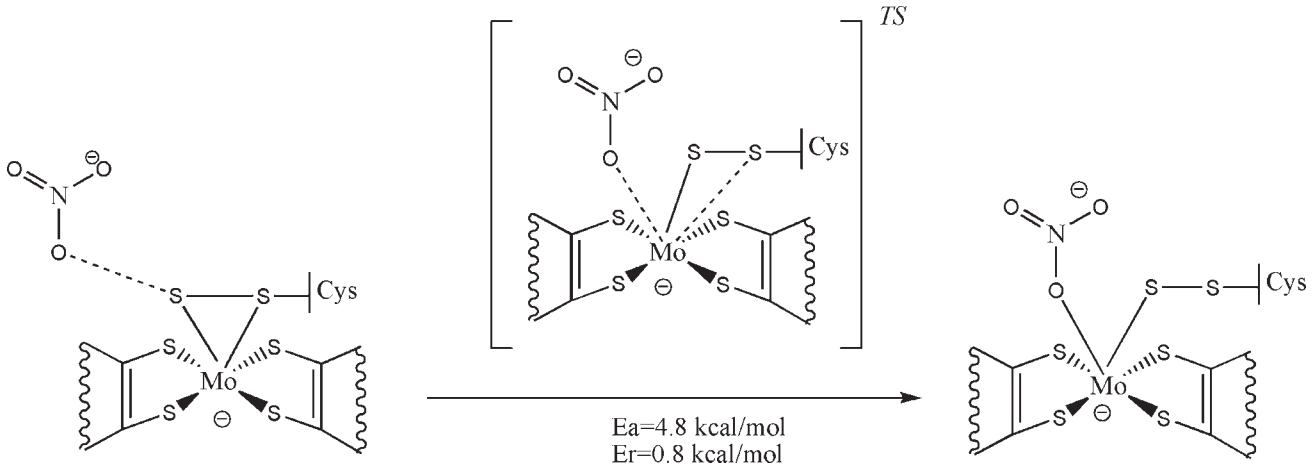

Scheme 3. Scheme of the first step of pathway 1 (Oxo-transfer reaction mediated by Mo^{VI}).

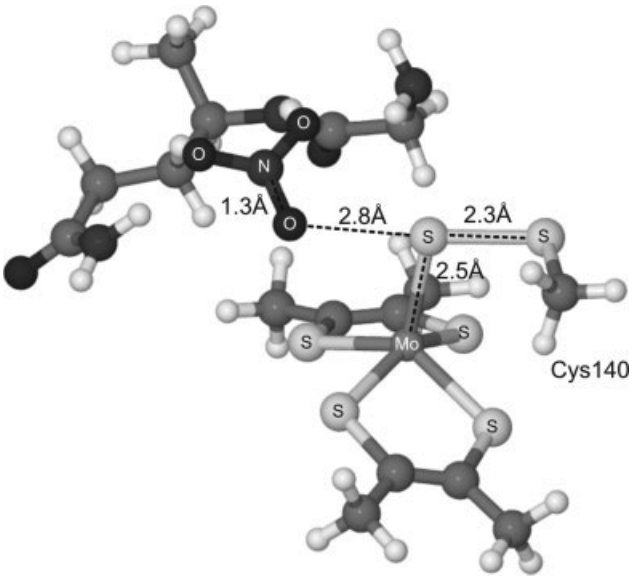

Figure 6. Optimized geometry of the transition state for step 1 from pathway 1.

of the nitrate promotes the stretching of the Mo-Cys140 bond to 3.7 Å, but the disulfide bridge retains an average value of 2.3 Å. The sulfur atom remains tightly bound to the molybdenum atom (2.50 Å) as in the reactants, but the charge becomes more concentrated in the dithiolene ligands (−0.73 a.u.) than in the molybdenum ion (−0.22 a.u.).

In the product of this reaction, the nitrate molecule maintains the planar geometry and becomes attached to the molybdenum atom (2.3 Å). The sulfur atom from Cys140 disconnects from the molybdenum (4.0 Å), but continues connected to the sulfur atom through a disulfide bridge (2.3 Å). The former remains connected to the molybdenum atom (2.4 Å) but no longer interact with the oxygen of the nitrate molecule (2.8 Å). The charge remain mainly in the molybdenum atom (−0.25 a.u.), the dithiolene ligands (−0.76 a.u.), and the nitrate molecule (−0.45 a.u.).

The overall energy of the reaction that involves the concomitant breaking of the Mo-S^{Cys140} bond and the formation of the (NO_2)-O-Mo(VI) bond requires a small activation energy of 4.8 kcal/mol and the reaction is almost thermo-neutral (0.82 kcal/mol) indicating that from the kinetic point of view this step is very favorable.

Step 2 (Scheme 4): The next step of the mechanism of pathway 1 involves the reduction of the nitrate into nitrite. The geometry of the reactants is similar to the products of the last step and the nitrate retains the planar geometry and connected to the molybdenum atom (2.3 Å). The sulfido remains connected to the molybdenum atom (2.4 Å) and to the Cys140 through a standard disulfide bridge (2.3 Å). The N-O bond length of the oxygen closer to the molybdenum atom is already slightly elongated (1.4 Å) and the charge is distributed mainly in the nitrate (−0.45 a.u.), the molybdenum atom (−0.25 a.u.) and the dithiolene ligands (−0.52 a.u.).

In the transition state the nitrate molecule adopts a trigonal pyramidal geometry, and the oxygen - molybdenum distance is shortened (1.9 Å) (Fig. 7). The nitrogen atom of the nitrate molecule is now closer to the sulfur atom at 3.1 Å, which is smaller than the sum of the Van der Waals radius of the N and S atoms. This interaction has a key role in the stabilization of the transition state geometry. The sulfur atom remains at 2.5 Å from the molybdenum atom and connected through a standard disulfide bridge to Cys140. Despite the conformational rearrangements observed in the products, the charge distribution did not change significantly compared to the reactants.

In the product of this reaction, the nitrite molecule is already formed and stays 6.1 Å away from the molybdenum center stabilized by the hydrogen bonds promoted by Gln346 and Gly454. The oxygen atom becomes firmly bound to the molybdenum atom (1.7 Å), the Mo-S bond length increases slightly to 2.6 Å and the sulfur atom remains connected through a disulfide bond to Cys140 (2.3 Å). The charge distribution is spread in the nitrite molecule (−0.62 a.u.) and the molybdenum complex

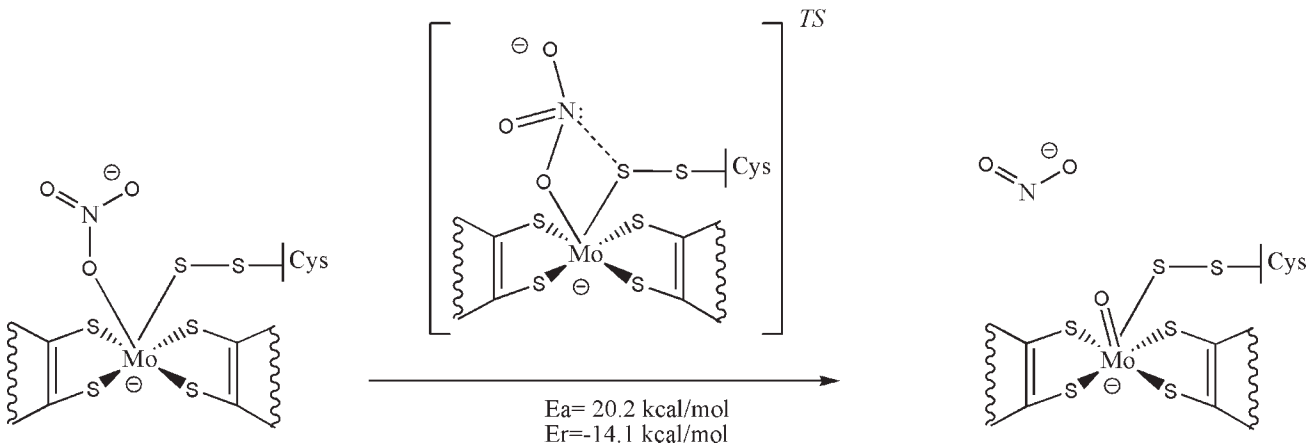

Scheme 4. Scheme of the second step of pathway 1 (Oxo-transfer reaction mediated by Mo^{VI}).

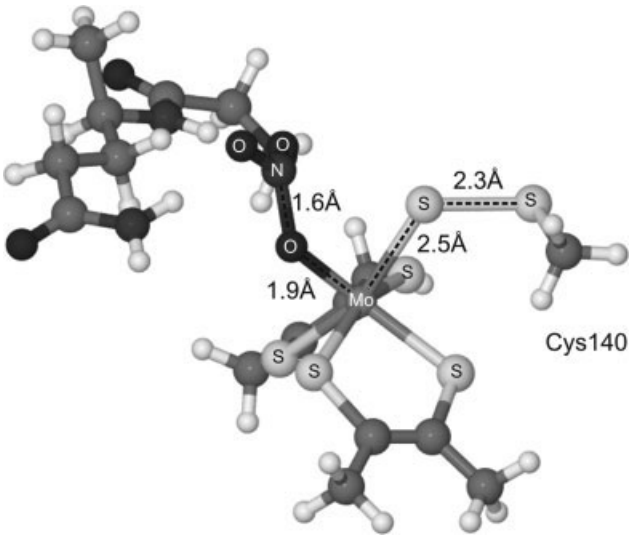

Figure 7. Optimized geometry of the transition state for step 2 from pathway 1.

(−0.85 Å). Due to the presence of the Mo = O bond, the charge is now more concentrated in the dithiolene ligands (−0.46 a.u.).

This reaction has activation energy of 20.2 kcal/mol and is exothermic in about −14.1 kcal/mol.

Oxo-Transfer Reaction Mediated by Mo^{V}bis(dithiolene)

Step 1 (Scheme 5): The geometry optimization of the Mo^{V} model kept the essential geometric features and hydrogen-bonding network observed in the crystal structure. The optimized geometry of the reactants was found to be distorted prismatic trigonal complex, with an average Mo-S(dithiolene) distance of 2.5 Å, an Mo-S^{Cys140} bond length of 2.6 Å, and an Mo-S bond length of 2.2 Å. The spin density is located at the molybdenum atom (0.98 a.u.), and the charge is spread between the nitrate molecule (−1.02 a.u.) the molybdenum, and its ligands. In the latter case, the charge is mainly concentrated on the molybdenum atom (−1.49 a.u.), in the sulfido (−0.76 a.u.), and in Cys140 (−0.61 a.u.). The sulfido and the Cys140 are close to each other by 3.3 Å, and considering the total charge of these two residues, it can be concluded that they interact with each other through an anionic disulfide bridge. In this minimum, the nitrate molecule adopts a planar geometry and interacts through several hydrogen bonds with the NH groups of Gln346 and Gly454 (average value of 2.0 Å). At this stage it only slightly interacts with the sulfur atom (5.28 Å) that is bonded to the molybdenum center.

In the transition state, the nitrate molecule slightly deviates from the planar geometry and is now found at 2.0 Å from the sulfide (Fig. 8). The interacting N-O bond length of the nitrate molecule slightly elongates from 1.3 Å to 1.4 Å, and the other two oxygens interact through hydrogen bonds with Gln346 and Gly454. The bond length between the molybdenum atom and the sulfur atom increased to 2.46 Å, but the bond length between the molybdenum atom and Cys140 remains almost unchanged (2.6 Å respectively). The same is also observed in the Mo-S(dithiolene) bond lengths (average values about 2.5 Å). As a consequence of this rearrangement, there is a slight redistribution of the charge in the system. The strength of the anionic disulfide bridge, formed by the sulfido and Cys140 in the reactants, is weakened (3.5 Å) and, looses the anionic character (0.02 a.u. and −0.27 a.u., respectively). As a consequence, the charge becomes spread within the bis(dimethyl dithiolene) ligands (1.21 a.u.), and not in the molybdenum atom as in the reactants (−0.39 a.u.). The spin density remains concentrated on the molybdenum atom.

In the products, the nitrate molecule becomes bonded to the sulfido (1.9 Å). Comparing with the geometry of the transition state structure, no substantial differences are found, and the sulfido and Cys140 remain distanced by 3.1 Å. The charge distribution remains concentrated in the bis(dimethyl dithiolene) ligands (1.21 a.u.) and in the nitrate molecule (−0.87 a.u.). The spin density remains concentrated on the molybdenum atom.

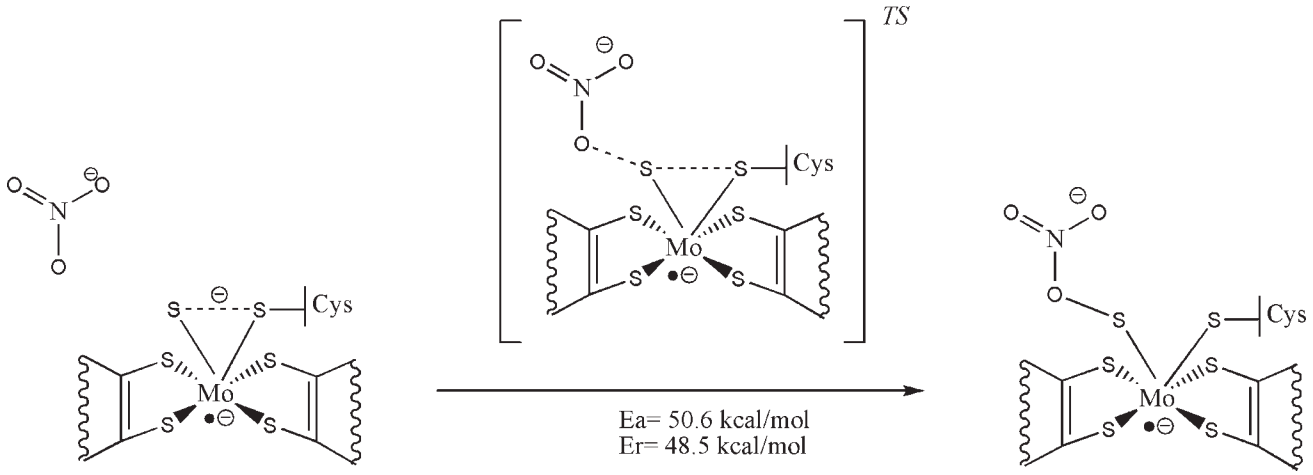

Scheme 5. Scheme of the first step of pathway 2 (Oxo-transfer reaction mediated by Mo^{V}).

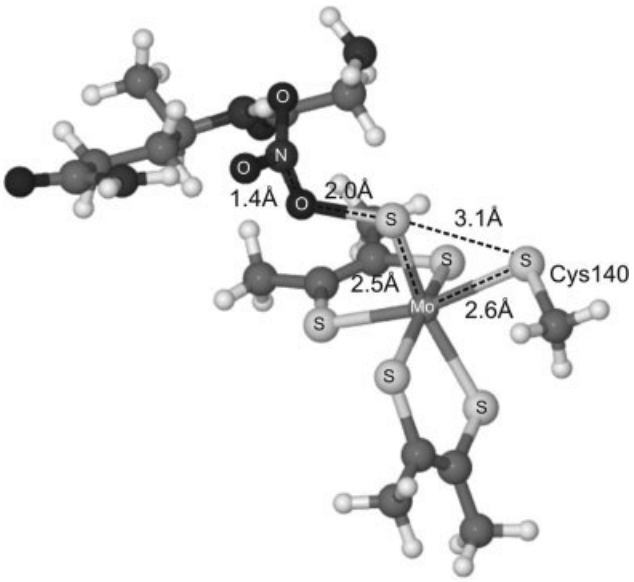

Figure 8. Optimized geometry of the transition state for step 1 from pathway 2.

It must be mentioned that the charge distribution observed in this step is crucial to allow the interaction of the nitrate molecule with the molybdenum center because the repulsion created by the presence of the negatively charged species would forbids this interaction. The bis(dimethyl dithiolene) ligands have an important role in charge dispersion and therefore favor the interaction with the nitrate molecule.

In spite of the charge redistribution observed in this step, the excess of negative charge does not favor it. This can be seen by the extremely high activation energy of 50.57 kcal/mol that the reaction requires and, the endothermicity of the reaction (48.47 kcal/mol), which turn this step very unfavorable. Despite the unfavorable energies obtained in this first step we followed this pathway till the formation of the nitrite molecule, to compare the overall mechanism with the Mo^{VI} pathway.

Step 2 (Scheme 6): The next step involves the formation of one nitrite molecule through the breaking of the NO bond of the nitrate molecule. The reactants are similar to the products obtained in the previous steps. The molybdenum atom is still bonded to the sulfido (2.5 Å) and to the Cys140 (2.6 Å). However, these two atoms no longer interact between each other (3.1 Å) due to the presence of the nitrate molecule that is bound to the sulfido (1.9 Å). The nitrate molecule retains the pyramidal conformation and is stabilized by several hydrogen bonds provided by Gln346 and Gly454. The charge is mainly located at the bis(dimethyl dithiolene) (1.21 a.u.) and in the nitrate molecule (−0.87 a.u.).

In the transition state, the NO bond increases to 2.0 Å (1.6 Å before) and, the distance between the oxygen and the sulfur is shortened to 1.8 Å (before 1.9 Å). As a consequence, the distance between the sulfur atom and Cys140 increases to 3.3 Å, but no significant changes are observed in the distance between these atoms and the molybdenum atom (Fig. 9). The spin density remains located in the molybdenum atom and the charge is still mostly distributed on the bis(dimethyl dithiolene) ligand (−1.25 a.u), and in the nitrate molecule (−0.90 a.u.).

In the products of this step, the distended N-O bond is broken and one nitrite molecule is obtained. The oxygen atom remains attached to the sulfido (1.8 Å) and, at the same time, to the molybdenum atom (1.9 Å). The nitrite molecule is stabilized by the hydrogen bonds promoted by the NH groups of Gln346 and Gly454 and is 5.8 Å away from the molybdenum complex. Cys140 is now far away from the sulfur atom (3.6 Å), but still in close contact to the molybdenum center (2.6 Å). The spin density continues focused on the molybdenum atom and the charge distribution mainly on the bis(dimethyl dithiolene) ligand (−1.08 a.u) and on the nitrite molecule (−0.66 a.u.).

Despite the unfavorable energies of the first step of this pathway the second step is very favorable due to the small activation energy of only 0.82 kcal/mol and to the large exothermicity of the reaction (−38.08 kcal/mol).

From this point two reactions can occur: The direct protonation of the oxygen that yields the water molecule, or the conformational rearrangement of Cys140 to yield a similar minimum

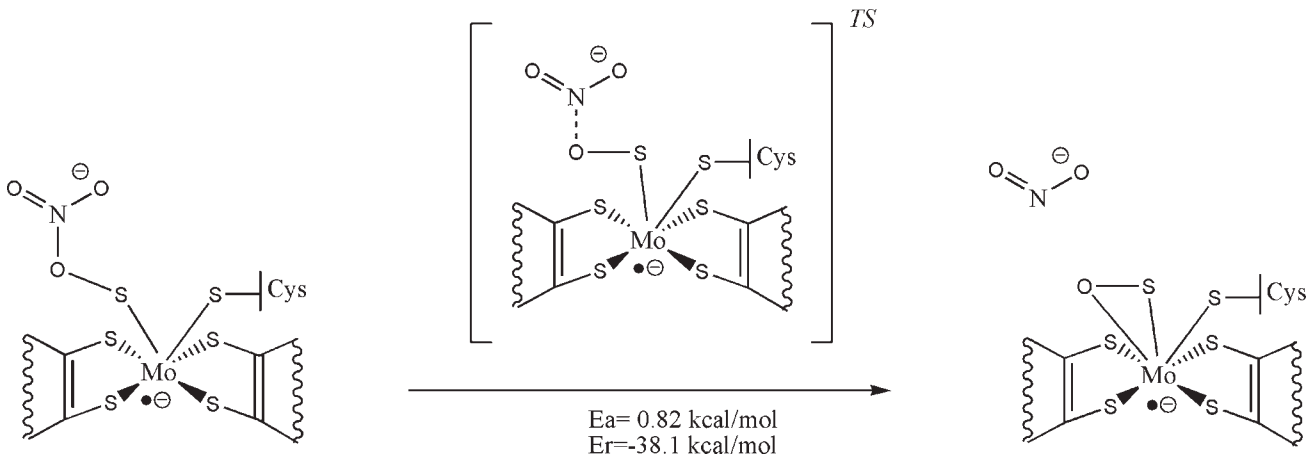

Scheme 6. Scheme of the second step of pathway 2(Oxo-transfer reaction mediated by Mo^{V}).

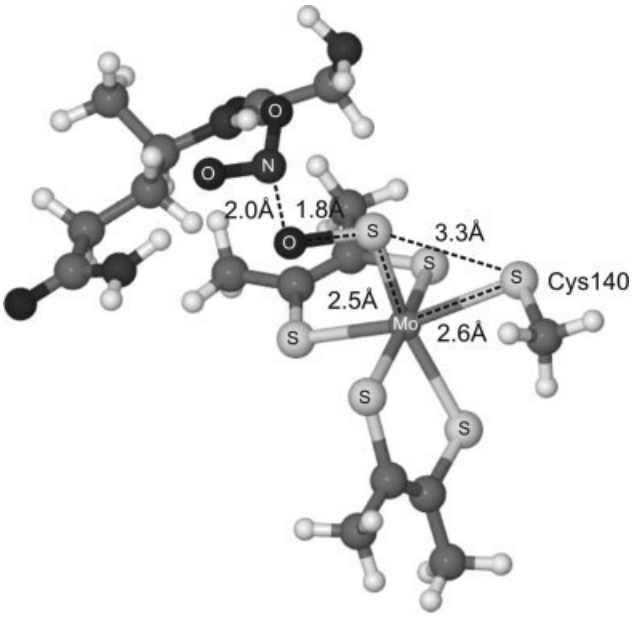

Figure 9. Optimized geometry of the transition state for step 2 from pathway 2.

to what was obtained with the Mo^{VI}. To test the second possibility we followed the reaction coordinate that involved the shortening of the distance between the sulfido and Cys140. The other possibility will be discussed in the next section.

Step3 (Scheme 7): The reactants are similar to the products of the last step, and the oxygen becomes attached to the molybdenum atom (1.9 Å) and, to the sulfido (1.3 Å). Despite this rearrangement the charge is mainly spread within the bis(dimethyl dithiolene) ligand (−1.08 a.u), and the spin density stays restricted to the molybdenum atom (0.96).

To obtain the transition state, we shortened the distance between the sulfido and Cys140 (Fig. 10). The transition state of this reaction shows the sulfido closer to Cys140 (2.3 Å), suggesting the formation of a disulfide bridge. The oxygen atom remains connected to the sulfido (2.3 Å), and to the molybdenum atom (2.0 Å). The charge remains concentrated on the dithiolenes attached to the molybdenum atom (−1.06 a.u.) and the spin on the molybdenum atom (0.99).

In the products of this reaction, we achieve a similar conformation to what was found with the Mo^{VI} model, but only after three sequential steps. The oxygen became bonded to the molybdenum atom through a double bound (1.7 Å), and Cys140 disconnects from the molybdenum atom (4.3 Å), but continues connected to the sulfido through a standard disulfide bridge (2.3 Å). The sulfido remains connected to the molybdenum center (2.7 Å) but no longer interacts with the oxygen atom (3.0 Å).

The charge remains concentrated on the dithiolene ligands attached to the molybdenum atom (−1.34 a.u.) and the spin on the molybdenum atom (0.98). This reaction requires an activation energy of +11.3 kcal/mol and the reaction is exothermic (−25.3 kcal/mol).

Discussion of the Most Favorable Oxidation State for Nitrate Binding and Reduction

As discussed before, in the absence of nitrate molecules the conformation adopted by the active site, with Mo^{V} or Mo^{VI}, is almost identical. The only difference is the nature of the disulfide bridge that connects the sulfido and Cys140, (in Mo^{V} it is an anionic disulfide bridge, while in Mo^{VI} it is a standard disulfide bridge). This is in agreement with the presence of a partial disulfide bond in the crystal structure[9] which was referred as being due to the partial reduction of the Mo center, a common occurrence due to exposure to X-rays.

The nitrate enters in the active site through a substrate accessing tunnel that is populated with several residues that drives it near the region where the molybdenum is located. Near the active site the tunnel becomes very narrow and does not allow the direct contact with the molybdenum atom, due to the presence of a pseudo-dithiolene ligand generated by the sulfido and Cys140. As a consequence the nitrate molecule can only interact directly with the sulfido, since the interaction with

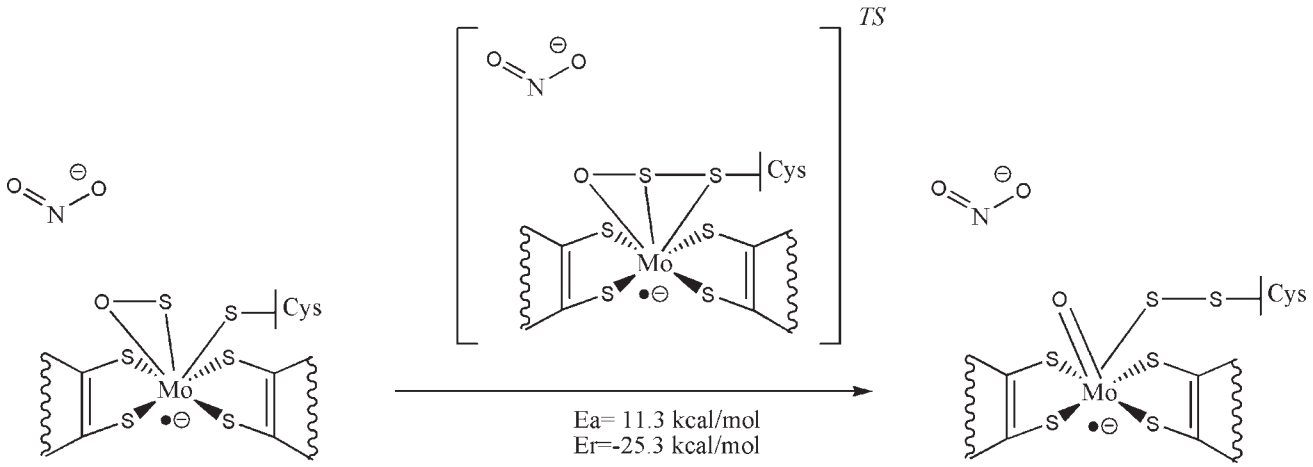

Scheme 7. Scheme of the third step of pathway 2 (Oxo-transfer reaction mediated by Mo^{V}).

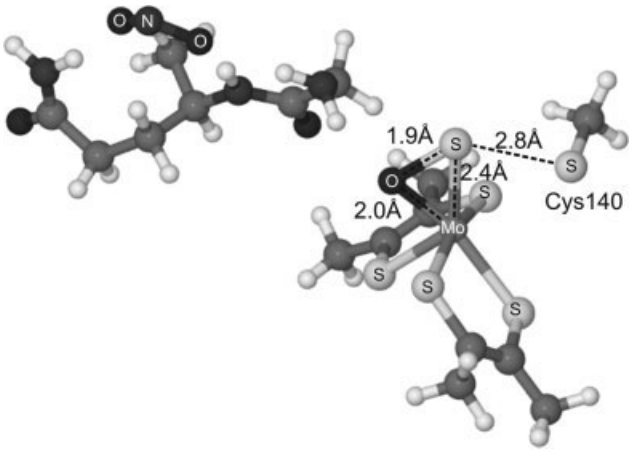

Figure 10. Optimized geometry of the transition state for step 3 from pathway 2.

Cys140 is blocked due to the presence of the neighboring residues.

The interaction of the nitrate molecule with the active site is not straightforward due not only to the narrow configuration of the active site, but also due to the negatively charged nitrate molecule and the molybdenum center that turn this approach unfavorable (specially on Mo^{V} species.). The interaction is only possible due to the presence of conserved Gln346 and Gly454 amino acids that stabilize the nitrate molecule in that region through several hydrogen bonds. This becomes clear analyzing the distance between them in the optimized structures of the reactants in the first step of both pathways (4–5 Å).

However, as the nitrate approaches to the sulfido, the reaction follows different pathways, depending on the oxidation state of the molybdenum. In Mo^{VI}, upon nitrate binding the active site undergoes a conformational rearrangement and the pseudo-dithiolene ligand shifts and opens a free access to the molybdenum ion. In the end of this step the nitrate molecule binds directly to the molybdenum ion, without a significant energetic cost (Ea = 4.8 kcal/mo and Er = 0.82 kcal/mol). In Mo^{V}, the presence of an extra electron in the system turns the approach more difficult. As a consequence, the first step involves the redistribution of the charge in the active site to promote the approach of the nitrate molecule. In this process, the bis(dimethyl dithiolene) ligands have an important role because they pour into them the excess of charge. Consequently, the anionic disulfide bond established between Cys140 and the sulfido is broken, which allows the binding of the nitrate molecule to the sulfido. This reaction does not lead to a significant conformational rearrangement of the complex but is very unfavorable from the energetic point of view, as it requires an extremely high activation energy (50.6 kcal/mol) and, the total reaction energy is highly endothermic (48.5 kcal/mol).

The nitrite molecule is produced in the second step of both mechanisms. In the pathway involving the Mo^{VI} ion, the step requires an activation of 20.2 kcal/mol and is exothermic in about −14.1 kcal/mol. In the products, the oxygen becomes double bonded to the molybdenum atom and Cys140 remains disconnected from the molybdenum atom. In the pathway involving the Mo^{V} ion, the nitrate molecule binds directly to the molybdenum atom without the breaking of the Mo-S and Mo_Cys140 bonds, oppositely to what is observed with Mo^{VI}. In the end of the second step, one nitrite molecule is produced and the oxygen becomes attached by a single bond to the molybdenum, together with the sulfido and Cys140, creating a heptacoordinated system. Despite the unfavorable energies of the first step, the second step of the pathway with Mo^{V} is very favorable due to the small activation energy of only 0.82 kcal/mol and to the large exothermicity of the reaction (−38.08 kcal/mol). Nevertheless the first step compromises the occurrence of the second step.

We have also studied if the Mo^{V} system tends to adopt a similar conformation to what was found with the Mo^{VI} system. The activation energy for this step is not very high (+11.3 kcal/mol) and the reaction is highly exothermic (−25.3 kcal/mol), which means that from the kinetic point of view the system tends to adopt that type of conformation.

The main difference between both minima is the charge distribution due to the presence of the extra electron on Mo^{V}.

These results show that the catalytic mechanism for the nitrate reduction into nitrite is more favorable with Mo^{VI} than with the Mo^{V}, as depicted in Figure 11. The energies involved in the steps are more favorable and the reduction process occurs in less steps, which from the kinetic point of view is an advantage.

The Mo^{V} mechanism is less feasible mostly due to the excess of the negative charge that precludes the approach of the nitrate molecule. The reaction was only possible due to the presence of the bis(dimethyl dithiolene) ligands that pour into them the excess of charge, allowing the molybdenum, the sulfido and Cys140 more available to react with the nitrate molecule. Once the nitrate becomes attached to the sulfido, the reaction is very favorable, despite the stereochemical hindrance that is created by the resulting heptacoordinated system.

In the Mo^{VI}, the system remains always hexacoordinated even in the initial steps. This occurs because once the nitrate approaches the active site the pseudo-dithiolene ligand adopts a conformational rearrangement that allows the direct access of nitrate to the molybdenum center. In this rearrangement Cys140 disconnects from the molybdenum and shifts to the region populated with several conserved methionines. The sulfido remains attached to the molybdenum and remains connected by a disulfide bridge with Cys140. The methionines have therefore also an important role in this mechanism because they stabilize the sulfur atom from Cys140 during the most part of the mechanism.

These results show that during the reduction process and regardless of the pathway that is followed, it is not the molybdenum that is oxidized, but the sulfido. This means that the chemistry involved in this process is a molybdenum/sulfur based redox chemistry and not only a redox chemistry based only on the Mo atom, as previously suggested.[6]

Regeneration of the Catalyst

The second part of the catalytic mechanism involves the formation of one water molecule and the subsequent enzymatic turnover. The available experimental data concerning this subject is

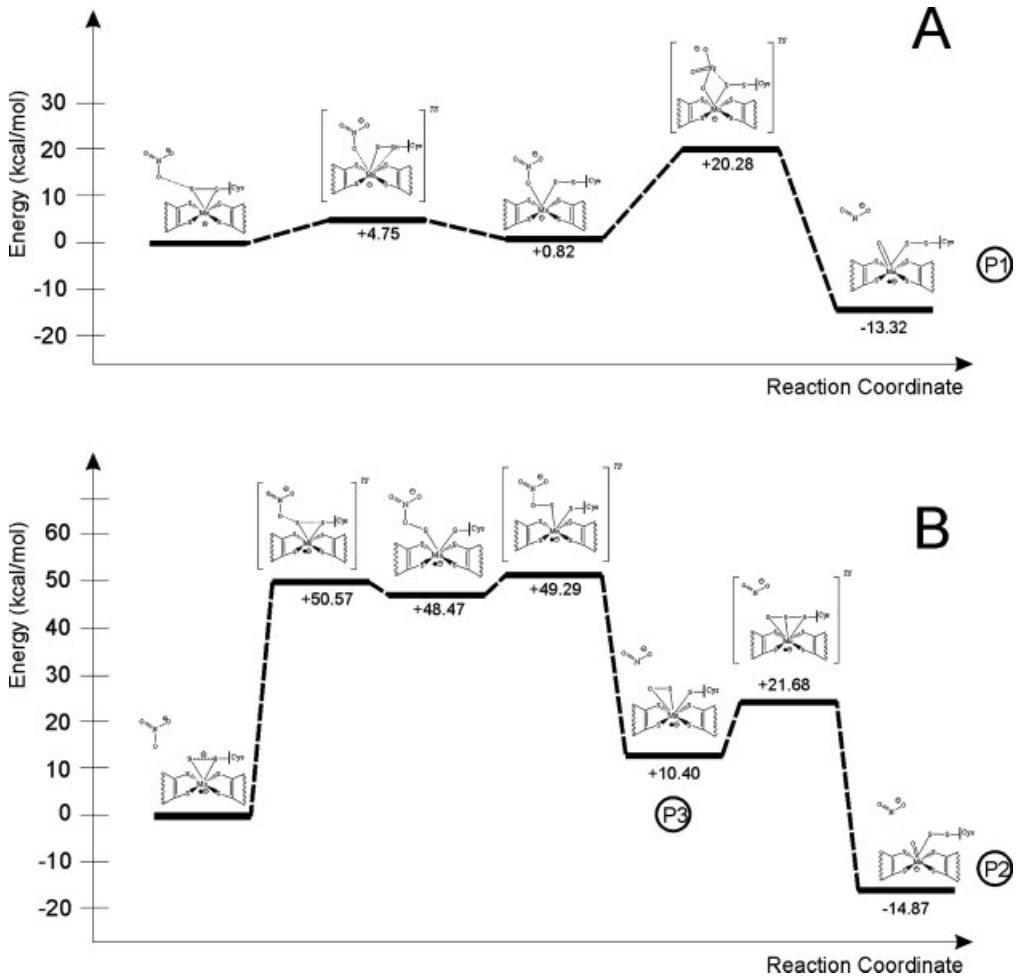

Figure 11. (A) Energetic pathway for oxo-tranfer with Mo^{VI} species. (B) Energetic pathway for oxo-tranfer with Mo^{V} species.

not conclusive, and it is accepted that two subsequent protonation steps addressed to the oxygen atom, concomitant with two electron transfer from the reductant, should occur.

From the two studied pathways, there are three possibilities for the protonation stage (Figure 11). Two of them have similar structures that only differ in the molybdenum oxidation state, i.e. P1 and P2. The third possibility involves the minimum obtained after the second step of pathway 2, where the oxygen becomes attached to the molybdenum atom together with the sulfur and Cys140, creating the heptacoordinated complex (P3).

The third possibility was afterwards discarded because the protonation of the oxygen atom leads to abnormal products where the molybdenum coordination sphere is destroyed. The other two possibilities maintain the coordination arrangement of the molybdenum complex and therefore are possible intervenients in the dehydration step.

The theoretical study of these reactions is a cumbersome issue because nothing is known about the source of the protons that are required to generate the water molecule and furthermore it is impossible to follow the two electron transfer from the reductants to the active site, by theoretical means.

Experimental studies performed by several authors[8,22–24] have shown that Mo^{V} and Mo^{VI} can be found in equilibrium. Taking into account the redox potential of the artificial electron donor (approximately -400 mV for methyl viologen), and the Nernst equation it can be concluded that the reduction of Mo^{VI} to Mo^{V} is highly favorable (-13.6 kcal/mol). Because the Mo^{V} minimum is more stable than the Mo^{VI} minimum it means that if electrons are available, the systems have a tendency to be reduced to Mo^{V} before the protonation stage. The reduction of Mo^{VI} to Mo^{V} is an important milestone for the following protonation steps because it favors the nucleophilic nature of the oxo-group and therefore catalyzes the gathering of protons from the surrounding environment.

The source of protons is also questionable and they can either be obtained from neighboring residues or from water molecules present near the active site. The presence of the two water channels (see Fig. 3) near the Mo center seems to support the second hypothesis, and therefore we simulated the protonation steps in the presence of water molecules. Taking this hypothesis into account and due to the impossibility to follow the kinetic of the dehydration mechanism we optimized the

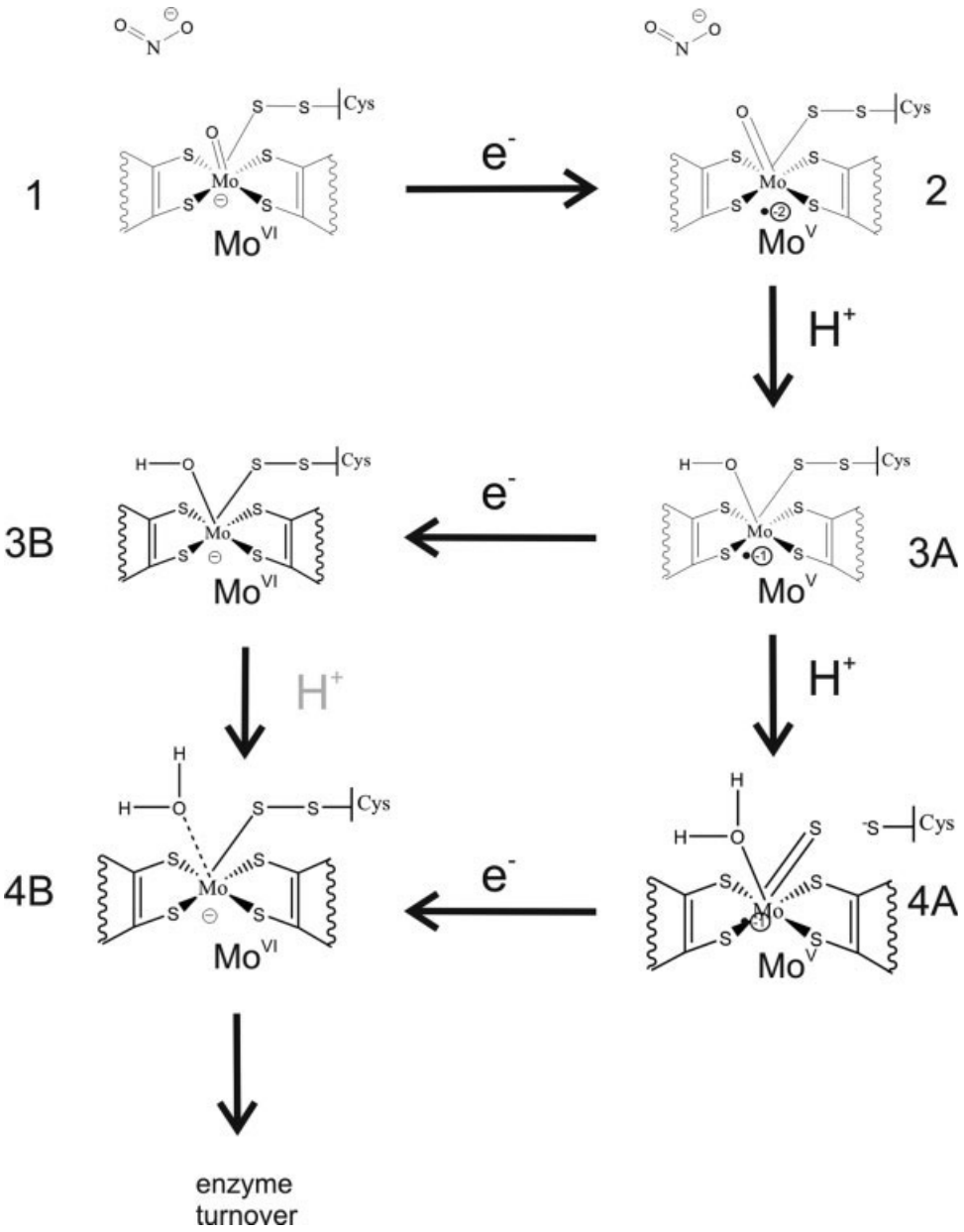

Figure 12. Optimized geometries of the products of the dehydration steps for the Mo^{VI} species.

structure of some possible intervenients that might be involved in the reaction (Figure 13 and Figure 14).

The first protonation step leads to the stretching of the Mo-O bond to 2.0 Å in Mo^{V} and 1.9 Å in Mo^{VI}. Also, it induces the shortening of the Mo-S bond to 2.6 Å in Mo^{V}, and 2.4 Å in Mo^{VI}. The second protonation step leads to the formation of one water molecule and the distance Mo-S is shortened to 2.5 Å in Mo^{VI} and 2.2 Å in Mo^{V}. The disulfide bond that connects the sulfido and Cys140 is maintained in Mo^{VI} (2.3 Å) but in Mo^{V} it is cleaved and Cys140 becomes negatively charged (0.80 a.u.), and distanced from the sulfide by 5.7 Å. As a consequence of this rearrangement, the water molecule remains attached to the molybdenum atom (2.2 Å) in Mo^{V}, precluding the enzyme turnover, while in the Mo^{VI}, the water molecule detach from the molybdenum atom (2.7 Å).

Taking into account these snapshots of the mechanism, we have created a possible pathway for the dehydration process, involving both Mo^{V} and Mo^{VI} species. The Mo^{V}, has one more electron than Mo^{VI}, and should increase the nucleophicity of the remaining oxo group and promote therefore its protonation. Accordingly, after nitrite releasing, the molybdenum is found as Mo^{VI} (Fig. 12, Compound **1**) requiring one electron to reduce to Mo^{V} (Figure 12, Compound **2**). If protons are readily available, the subsequent protonation should occur without a high energetic

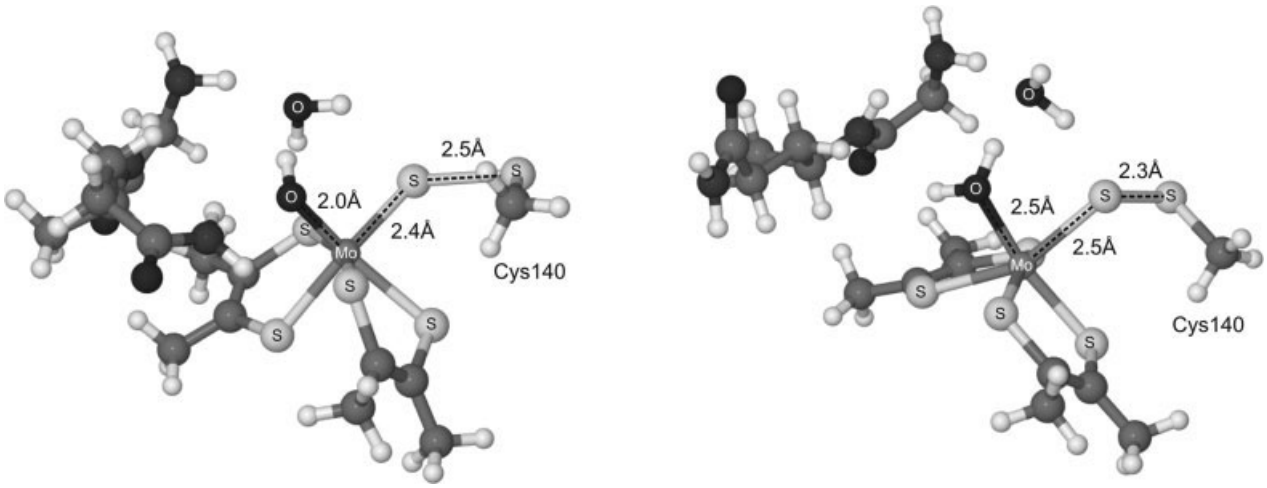

Figure 13. Optimized geometries of the products of the dehydration steps for the Mo^{V} species.

cost leading to compound **3A** of Figure 12. If electrons are now available the molybdenum tends to be found as Mo^{VI}, generating compound **3B** of compound 8. Otherwise, if electrons are unavailable the system will follow for the second protonation, generating compound **4A** from Figure 12.

This minimum does not allow for the enzyme turnover because the water molecule remains attached to the molybdenum. Therefore the system will be blocked till one electron is pumped to the active site. Once this is available the system will tend for compound **4B** Figure 12 that leads to water dissociation and the concomitant enzyme turnover. Another possibility would involve protonation of compound **3B** Figure 12 that would instantly induce the water dissociation and therefore enzyme turnover. We believe that both species **3A** and **3B** should be equally found in solution if electron and protons are available.

The Mo^{V} intermediates obtained after electron donor shortage by EPR spectroscopy in the DdNapA,[9,22] suggest that the interacting protons could be bound either to the sulfido group, as a water molecule placed in the second coordination sphere of molybdenum, or as a water molecule directly coordinated to the molybdenum atom. This latter possibility might also imply the loss of the bond between the Cys and the molybdenum, because no hyperfine couplings associated with the b-methylene protons from the Cys were detected. Comparing this result with the proposed mechanism we propose that this signal belongs to structure **4A** of Figure 12. Taking in account these results we propose that the EPR signals are a consequence of the absence of

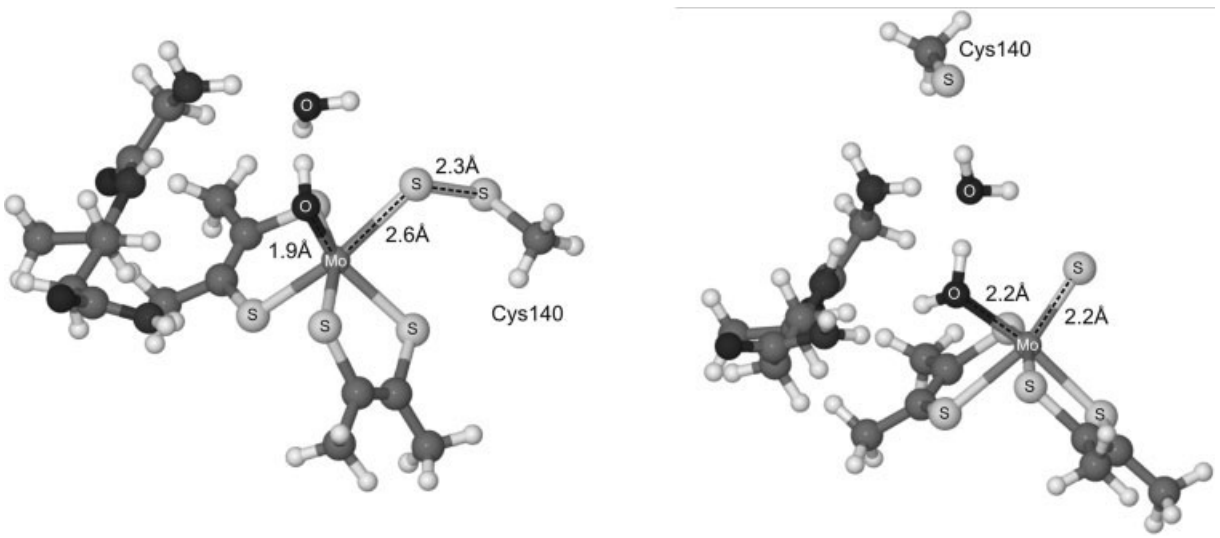

Figure 14. Mechanism of the dehydration pathway.

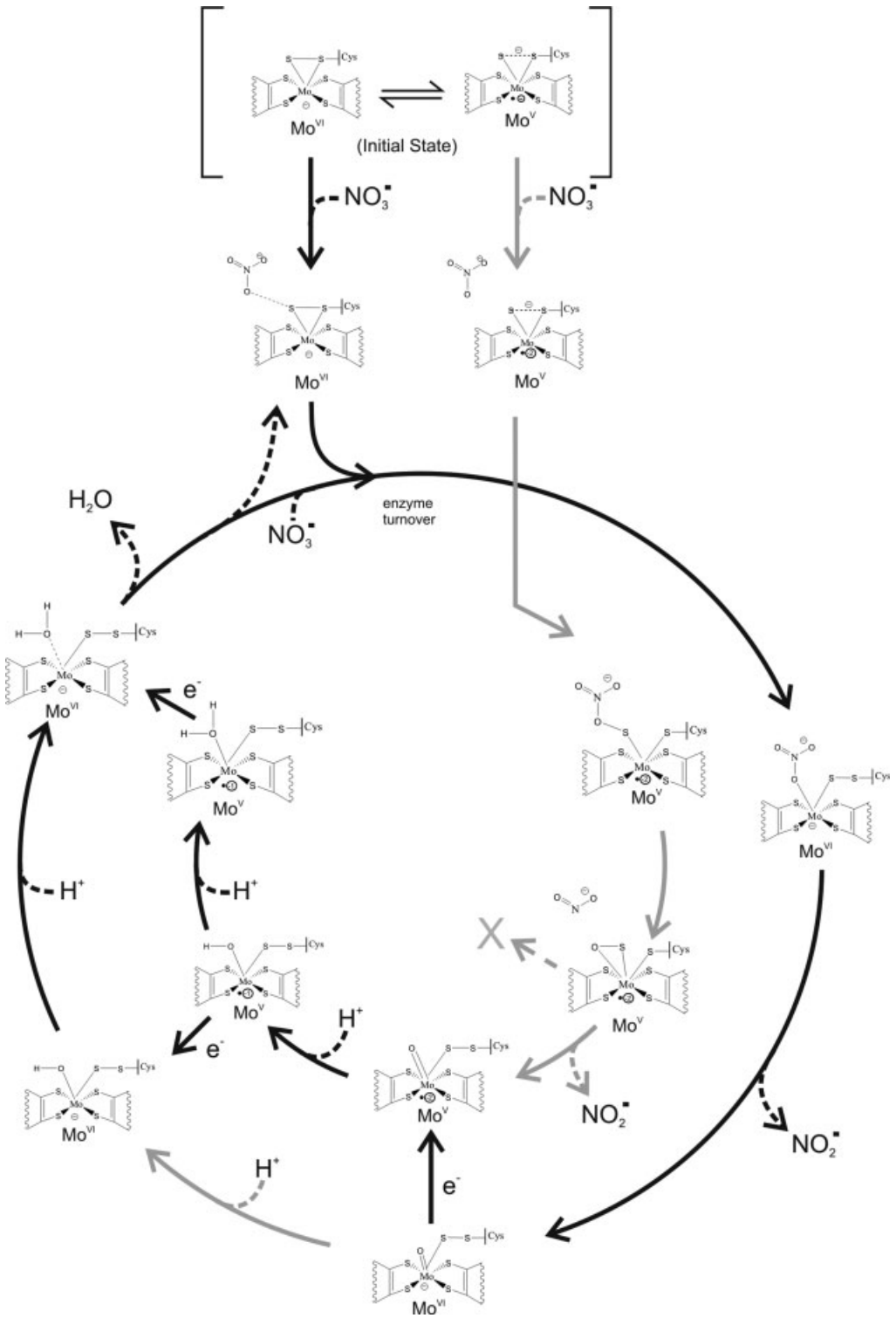

Scheme 8. Schematic representation of the studied mechanisms that lead to the nitrate reduction into nitrite and enzyme turnover (Black—most favorable pathway; grey—less favorable pathway).

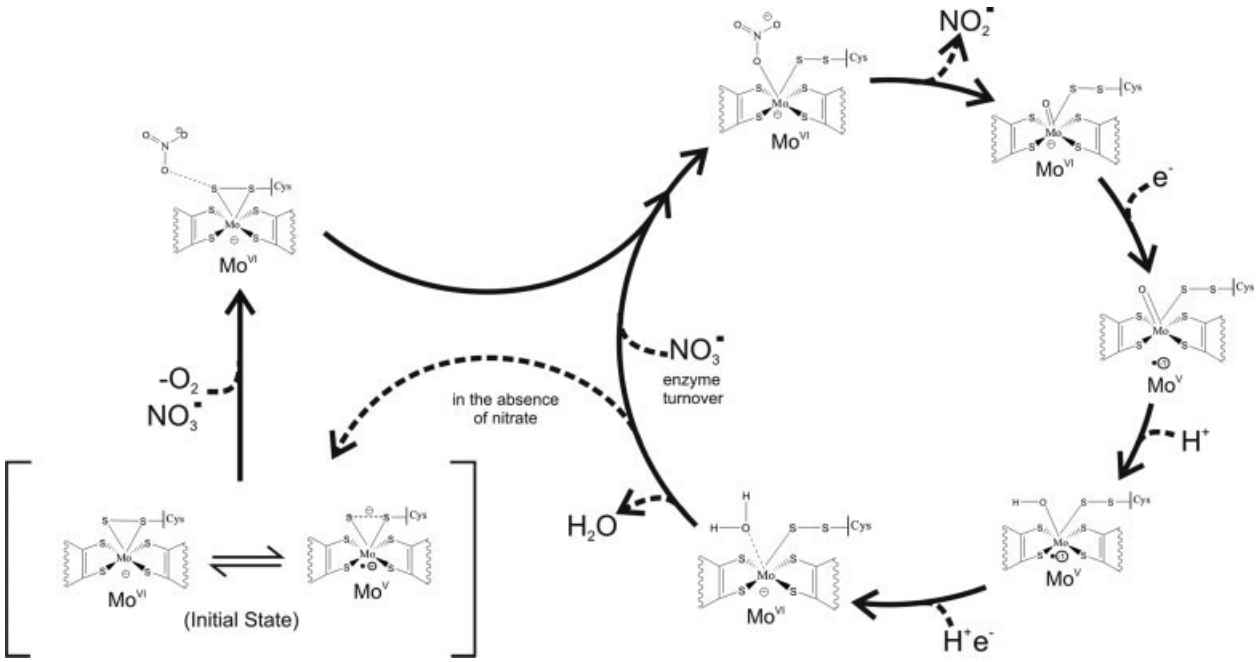

Scheme 9. Catalytic mechanism of periplasmic nitrate reductase proposed in this article.

electrons that block the catalytic cycle leading to the accumulation of compound **4A** in solution.

Conclusions

The catalytic mechanism of nitrate reduction into nitrite has been a subject under intense research in the last years. Many proposals are available in the literature, based on theoretical and experimental data.[6,8,9,30] However, the recent discover that there is a sulfur atom present in the molybdenum coordination sphere, together with the new electrochemistry and EPR studies demanded a reevaluation of the catalytic mechanism. Most of the mechanisms reported in the literature for related nitrate reductases have been based on the scheme indicated by Dias et al.[6] Recent electrochemistry studies have shown however that the potential over which Mo^{V} is reduced to Mo^{VI} is below −400 mV (vs. SHE) which cannot be obtained from physiological reductants.[8] As the redox potential necessary to reduce Mo^{VI} to Mo^{V} is between +200 and −200 mV it means that both redox states can be found in equilibrium and should be species involved in the mechanism of substrate binding *in vivo*.

The theoretical and computational studies performed in this study have shown that both species have an active role on the mechanism but in different phases. The Mo^{VI} is required for the nitrate reduction into nitrite. The Mo^{V} is involved in the second part of the mechanism where one water molecule is formed and enzyme turnover occurs. The new proposal of the mechanism is depicted in Scheme 8.

In the absence of nitrate the molybdenum can be found in equilibrium as Mo^{V} or Mo^{VI}. The change in the molybdenum redox states does not change the configuration of the active site as previously proposed,[9] and the sulfido and Cys140 remain attached to the molybdenum atom. The only difference is that in Mo^{VI} these ligands are connected by a standard disulfide bridge, while in Mo^{V} they are bound by an anionic disulfide bridge.[31]

Once the nitrate molecule reaches the substrate accessing tunnel it is guided/attracted by several conserved amino acids (Arg354, Asp155, Glu156, and Asp355) to the active site where the molybdenum is located (12 Å below the molecular surface). The access of the nitrate molecule to this center in not straightforward because the tunnel becomes very narrow near that region and it can only interact with the sulfido that is attached to the molybdenum. The direct contact with Cys140 is precluded due to the active site configuration. Moreover, the sulfido and Cys140 create a pseudo-dithiolene ligand that blocks any direct contact of the nitrate with the molybdenum atom. This protection may be used by the enzyme to protect the molybdenum from the solvent and by other small molecules that could destroy the active site or to impair electron pump from external oxidants. Another factor that does not favor the nitrate approach is the repulsion that is induced by the molybdenum center since it is also negatively charged. The presence of the nitrate molecule near the active site is only possible due to the presence of the conserved amino acids Gln346 and Gly345 that stabilize it through several hydrogen bonds.

The nitrate reduction into nitrite is only favorable with the Mo^{VI} system. As the nitrate interacts with the sulfur atom it induces a conformational rearrangement of the active site and Cys140 disconnects from the molybdenum and moves towards the region populated with several methionines. The terminal sulfur atom remains attached to the molybdenum atom but this rearrangement is sufficient to open free access for the nitrate molecule to the molybdenum atom. The nitrate becomes directly

bonded to the molybdenum atom and with an activation energy of 20.2 kcal/mol the nitrite molecule is formed and the oxygen becomes bonded to the molybdenum by a double bond. In this reduction process it is not the molybdenum that is oxidized but it is the terminal sulfur atom, contrasting to what was previously proposed.[6] The bis(dimethyl dithiolene) ligands have a preponderant role in this step since they spread the negative charge and promote the conformational rearrangement of the active site that is required for the reaction of nitrate with the molybdenum atom. The step is exothermic in 14.1 kcal/mol and the overall configuration of the active site remains unchanged. Cys140 remains disconnected from the molybdenum and should remain in close contact with the neighboring methionine residues. These residues have also a relevant role in this step since they promote the stabilization of Cys140 that is also essential for the reaction.

The second part of the mechanism involves the formation of a water molecule and subsequent enzyme turnover. In this step we proposed that the proton should be readily available since two water channels are present and directed to the molybdenum center. However the Mo^{VI} species might not be a sufficient nucleophile to assist the protonation steps. Therefore we propose that the molybdenum must be reduced to Mo^{V} and therefore one electron is required from external reductants. Taking in account the redox potential of the reductants and of the Mo^{V}/Mo^{VI} couple, this step would be very favorable (around -8.5 kcal/mol).

From this point two pathways are possible that lead to the formation of the water molecule. If the electron transfer is slower than the protonation steps, then both protonation steps occur in the presence of Mo^{V} species. Otherwise, the first protonation step takes place with Mo^{V}, and thereafter one electron will be pumped into the active site leading to the Mo^{VI} intermediate, that undergo the second protonation step. The available experimental data is not sufficient to reveal which pathways is the most favorable and therefore we believe that both of them can occur. Only the availability of protons and electrons might dictate which pathway will be favored, as it was observed with the EPR experiments performed by Gonzalez et al.[22] where the shortage of electrons favored the presence of Mo^{V} species.

Independent of the followed pathway, the computational results have shown that the water elimination and therefore the concomitant enzyme turnover can only occur with Mo^{VI} species. This means that if the protonation occur with the Mo^{V} species the second electron must be pumped to the active site after the protonation stage.

Once the water molecule dissociates from the active site the enzymatic turnover can occur by two different pathways. If the conformational rearrangement of the active site remains unaltered then the first step of the mechanism is not necessary and the nitrate molecule would bind directly to the molybdenum atom. If the sulfido and Cys140 return to their initial positions, they block the access to the molybdenum atom and consequently to start a new reduction process it is required a new conformational rearrangement of these atoms with an energetic cost of 4.8 kcal/mol (dashed arrow in Scheme 8). We propose that if nitrate molecules are available near the active site, the channel should remain opened till no more nitrate molecules are available. This pressure will also promote the water elimination through the water channels, and turn the reduction process more efficient. In the absence of nitrate molecules, Cys140 and the sulfido should return to their initial positions, closing by this way the free access to the molybdenum atom. This conformation should be maintained by the enzyme to protect the active site from the solvent, until new nitrate molecules become available. Scheme 9 summarizes the proposed catalytic mechanism for nitrate reduction into nitrite.

Further crystallographic studies are being done on different forms of the enzyme and the data will allow further confirmation at least for some of the relevant catalytic intermediates.

References

1. Moura, J. J. G.; Brondino, C. D.; Trincao, J.; Romao, M. J. J Biol Inorg Chem 2004, 9, 791.
2. Gonzalez, P. J.; Correia, C.; Moura, I.; Brondino, C. D.; Moura, J. J. G. J Inorg Biochem 2006, 100, 1015.
3. Hille, R. Chem Rev 1996, 96, 2757.
4. Richardson, D. J.; Berks, B. C.; Russell, D. A.; Spiro, S.; Taylor, C. J. Cell Mol Life Sci 2001, 58, 165.
5. Fischer, K.; Barbier, G. G.; Hecht, H. J.; Mendel, R. R.; Campbell, W. H.; Schwarz, G. Plant Cell 2005, 17, 1167.
6. Dias, J. M.; Than, M. E.; Humm, A.; Huber, R.; Bourenkov, G. P.; Bartunik, H. D.; Bursakov, S.; Calvete, J.; Caldeira, J.; Carneiro, C.; Moura, J. J. G.; Moura, I.; Romao, M. J. Structure 1999, 7, 65.
7. Arnoux, P.; Sabaty, M.; Alric, J.; Frangioni, B.; Guigliarelli, B.; Adriano, J. M.; Pignol, D. Nat Struct Biol 2003, 10, 928.
8. Jepson, B. J. N.; Mohan, S.; Clarke, T. A.; Gates, A. J.; Cole, J. A.; Butler, C. S.; Butt, J. N.; Hemmings, A. M.; Richardson, D. J. J Biol Chem 2007, 282, 6425.
9. Najmudin, S.; Gonzalez, P. J.; Trincao, J.; Coelho, C.; Mukhopadhyay, A.; Cerqueira, N. M. F. S. A.; Romao, C. C.; Moura, I.; Moura, J. J. G.; Brondino, C. D.; Romao, M. J. J Biol Inorg Chem 2008, 13, 737.
10. Raaijmakers, H.; Macieira, S.; Dias, J. M.; Teixeira, S.; Bursakov, S.; Huber, R.; Moura, J. J. G.; Moura, I.; Romao, M. J. Structure 2002, 10, 1261.
11. Raaijmakers, H. C. A.; Romao, M. J. J Biol Inorg Chem 2006, 11, 849.
12. Frisch, M. J.; Trucks, G. W.; Schlegel, H. B.; Scuseria G. E.; Robb, M. A.; Cheeseman, J. R.; Zakrzewski, V. G.; Montgomery, J. A., Jr.; Stratmann, R. E.; Burant, J. C.; Dapprich, S.; Millam, J. M.; Daniels, A. D.; Kudin, K. N.; Strain, M. C.; Farkas, O.; Tomasi, J.; Barone, V.; Cossi, M.; Cammi, R.; Mennucci, B.; Pomelli, C.; Adamo, C.; Clifford, S.; Ochterski, J.; Petersson, G. A.; Ayala, P. Y.; Cui, Q.; Morokuma, K.; Malick, D. K.; Rabuck, D. A.; Raghavachari, K.; Foresman, J. B.; Cioslowski, J.; Ortiz, J. V.; Baboul, A. G.; Stefanov, B. B.; Liu, G.; Liashenko, A.; Piskorz, P.; Komaromi, I.; Gomperts, R.; Martin, R. L.; Fox, D. J.; Keith, T.; Al-Laham, M. A.; Peng, C. Y.; Nanayakkara, A.; Gonzalez, C.; Challacombe, M.; Gill, P. M. W.; Johnson, B.; Chen, W.; Wong, M. W.; Andres, J. L.; Gonzalez, C.; Head-Gordon, M.; Replogle, E. S.; Pople, J. A. Gaussian, Inc.: Pittsburgh, PA, 2003.
13. Becke, A. D. J Chem Phys 1993, 98, 5648.
14. Lee, C. T.; Yang, W. T.; Parr, R. G. Phys Rev B 1988, 37, 785.
15. Vosko, S. H.; Wilk, L.; Nusair, M. Can J Phys 1980, 58, 1200.
16. Stephens, P. J.; Devlin, F. J.; Chabalowski, C. F.; Frisch, M. J. J Phys Chem 1994, 98, 11623.
17. Hay, P. J.; Wadt, W. R. J Chem Phys 1985, 82, 299.

18. Cerqueira, N. M. F. S. A.; Femandes, P. A.; Eriksson, L. A.; Ramos, M. J. J Mol Struc-Theochem 2004, 709, 53.
19. Cerqueira, N. M. F. S. A.; Fernandes, P. A.; Eriksson, L. A.; Ramos, M. J. Biophys J 2006, 90, 2109.
20. Himo, F. Theor Chem Acc 2006, 116, 232.
21. Brondino, C. D.; Rivas, M. G.; Romao, M. J.; Moura, J. J. G.; Moura, I. Acc Chem Res 2006, 39, 788.
22. Gonzalez, P. J.; Rivas, M. G.; Brondino, C. D.; Bursakov, S. A.; Moura, I.; Moura, J. J. G. J Biol Inorg Chem 2006, 11, 609.
23. Frangioni, B.; Arnoux, P.; Sabaty, M.; Pignol, D.; Bertrand, P.; Guigliarelli, B.; Leger, C. J Am Chem Soc 2004, 126, 1328.
24. Jepson, B. J. N.; Anderson, L. J.; Rubio, L. M.; Taylor, C. J.; Butler, C. S.; Flores, E.; Herrero, A.; Butt, J. N.; Richardson, D. J. J Biol Chem 2004, 279, 32212.
25. Petřek, M.; Otyepka, M.; Banáš, P.; Košsinová, P.; Koča, J.; Damborský, J. BMC Bioinformatics 2006, 7, 316.
26. Damborský, J.; Petřek, M.; Banáš, P.; Otyepka, M. Biotechnol J 2007, 2, 62.
27. Damborský, J.; Petřek, M.; Banáš, P.; Otyepka, M. Biotechnol J 2007, 2, 62.
28. Butler, C. S.; Charnock, J. M.; Bennett, B.; Sears, H. J.; Reilly, A. J.; Ferguson, S. J.; Garner, C. D.; Lowe, D. J.; Thomson, A. J.; Berks, B. C.; Richardson, D. J. Biochem 1999, 38, 9000.
29. Leopoldini, M.; Russo, N.; Toscano, M.; Dulak, M.; Wesolowski, T. A. Chemistry—Eur J 2006, 12, 2532.
30. Hofmann, M. J Biol Inorg Chem 2007, 12, 989.
31. Stiefel, E. I. J Chem Soc Dalton Trans 1997, 21, 3915.